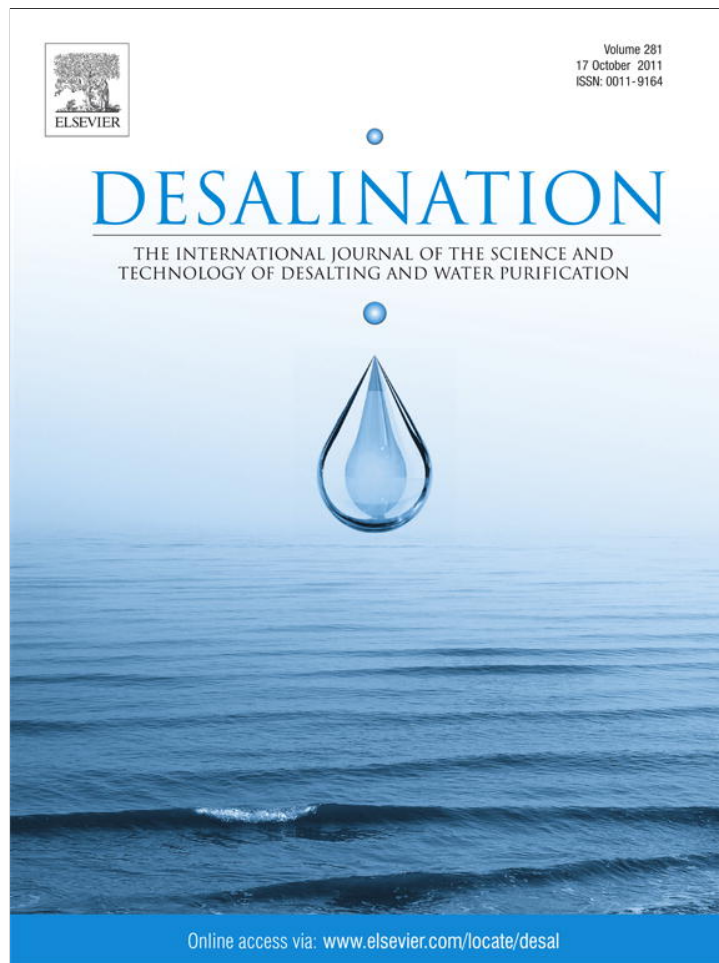


Provided for non-commercial research and education use.  
Not for reproduction, distribution or commercial use.



This article appeared in a journal published by Elsevier. The attached copy is furnished to the author for internal non-commercial research and education use, including for instruction at the authors institution and sharing with colleagues.

Other uses, including reproduction and distribution, or selling or licensing copies, or posting to personal, institutional or third party websites are prohibited.

In most cases authors are permitted to post their version of the article (e.g. in Word or Tex form) to their personal website or institutional repository. Authors requiring further information regarding Elsevier's archiving and manuscript policies are encouraged to visit:

<http://www.elsevier.com/copyright>



Contents lists available at ScienceDirect

Desalination

journal homepage: [www.elsevier.com/locate/desal](http://www.elsevier.com/locate/desal)

## PEI-grafted magnetic porous powder for highly effective adsorption of heavy metal ions

Ya Pang, Guangming Zeng\*, Lin Tang\*, Yi Zhang, Yuanyuan Liu, Xiaoxia Lei, Zhen Li, Jiachao Zhang, Gengxin Xie

College of Environmental Science and Engineering, Hunan University, Changsha, 410082, China

Key Laboratory of Environmental Biology and Pollution Control (Hunan University), Ministry of Education, Changsha, 410082, China

### ARTICLE INFO

#### Article history:

Received 19 April 2011

Received in revised form 1 August 2011

Accepted 2 August 2011

Available online 24 August 2011

#### Keywords:

Magnetic adsorbent

PEI

Heavy metals

Adsorption

### ABSTRACT

The aim of this study is to develop a polyethylenimine (PEI) grafted magnetic porous adsorbent for highly effective adsorption of heavy metals. The process of grafting PEI was confirmed by Fourier transform infrared (FTIR) analysis. Batch tests were carried out to investigate the adsorption performance. Adsorption of  $\text{Cu}^{2+}$ ,  $\text{Zn}^{2+}$  and  $\text{Cd}^{2+}$  was dependent on pH and increasing the pH was favorable to metal ions removal. The adsorption equilibrium was reached within 10 min and well described by pseudo-second-order model. The sorption isotherms of the adsorbent for these metals fitted well with Langmuir model, with maximum adsorption capacities of 157.8, 138.8 and 105.2 mg/g for  $\text{Cu}^{2+}$ ,  $\text{Zn}^{2+}$  and  $\text{Cd}^{2+}$ , respectively. Competitive adsorption among the three metal ions showed a preferential adsorption of  $\text{Cu}^{2+} > \text{Zn}^{2+} > \text{Cd}^{2+}$ . The magnetic adsorbent exhibited excellent acid–alkali stability. In addition, the exhausted adsorbent can be regenerated by 0.02 mol/L EDTA solution without significant adsorption capacity loss.

© 2011 Elsevier B.V. All rights reserved.

### 1. Introduction

Heavy metals pollution is commonly found in waste water of many industrial processes and has been known to cause severe threat on the public health and ecological systems [1,2]. Adsorption is one of the most popular and effective methods for heavy metals pollution remediation, due to the adsorption process offers flexibility in design and operation. And the treated effluent is reusable in many cases. In addition, the regeneration of adsorbent with economic operation may be possible because adsorption is general reversible [3,4]. Various adsorbents are developed to effectively remove heavy metal ions from effluent, such as cheap and abundant cellulose and its modified forms [1], natural and modified kaolinite and montmorillonite [5], synthesized hydrogels [6], as well as multifarious agricultural waste material and potentially low cost sorbents [7,8].

The application of magnetic adsorbent to solve the water pollution has attracted widespread interest [9], for it can be separated from the aqueous solution by applying an external magnetic field instead of centrifugation or filtration. The magnetic adsorbent can be made into a porous structure, whose presence increases the surface area, reduces diffusion resistance and facilitates mass transfer [10]. A new mesoporous  $\text{Fe}_7\text{Co}_3$  carbon nanocomposite synthesized via simple

casting method displayed high adsorption capacity for methylene blue trihydrate (458 mg/g) [10]. Besides introducing magnetism and porous structure, surface modification is one of the most effective and widely used methods to enhance the adsorption capacity. For instance, Wang et al. reported that the adsorption capacities of  $\text{Fe}_3\text{O}_4/\text{SiO}_2$  nanoparticles were increased significantly after the modification of amino groups [11]. Lam et al. noted that  $\text{NH}_2$ -MCM-41 and SH-MCM-41 adsorbents, which were prepared by grafting aminopropyl and thiolpropyl groups onto the MCM-41 mesoporous silica, displayed strong affinity for gold in waste water [12]. Among these researches, the introduced functional groups like carboxylate, hydroxyl, sulfate and amino groups on the matrix surface are responsible for heavy metal sorption, due to their affinity for heavy metal ions to form metal complexes or chelates [7]. Therefore, selecting a functional material to modify the matrix is of great importance in developing high performance magnetic adsorbent.

Polyethylenimine (PEI), which is composed of plenty of amine groups on the line type macromolecular chains, exhibits strong adsorption ability for heavy metals. However, because of the water soluble nature of PEI, it has to be immobilized on matrix to ensure the maneuverability when used as adsorbent. Insoluble polymers [13,14], biomass [15,16] and cellulose [17] have been used to crosslink PEI to prevent its leaching during adsorption operation. Silica, which is low cost and stable, has been applied to immobilize PEI for effective removal of heavy metals [18–21]. However, the silica-based adsorbent suffered from relatively long time to reach adsorption equilibrium, and its separation was relatively complex.

\* Corresponding authors at: College of Environmental Science and Engineering, Hunan University, Changsha 410082, China. Tel.: +86 731 88822754; fax: +86 731 88823701.

E-mail addresses: [zgming@hnu.cn](mailto:zgming@hnu.cn) (G. Zeng), [tanglin@hnu.cn](mailto:tanglin@hnu.cn) (L. Tang).

This paper focuses on preparing a PEI modified magnetic porous adsorbent for effective adsorption of heavy metals. A magnetic porous powder composed of  $\text{SiO}_2$  and  $\text{Fe}_3\text{O}_4$  was prepared by dispersion polymerization method, on which PEI was grafted to develop the PEI-grafted magnetic porous adsorbent. The resultant adsorbent was characterized and its adsorption behaviors including kinetics, sorption isotherm, competitive adsorption and stability of this adsorbent were estimated.

## 2. Materials and methods

### 2.1. Preparation of magnetic porous composite

The magnetic nanoparticles  $\text{Fe}_3\text{O}_4$  were first synthesized by conventional chemical coprecipitation method [22]. Then  $\text{SiO}_2$  sol was prepared using tetraethyl orthosilicate (TEOS), ethanol, water and nitric acid with the molar ratio of 1:3.8:6.4:0.085. The next was preparation of the magnetic porous composite, in short, an amount of 40 g urea was dissolved in 250 mL prepared  $\text{SiO}_2$  sol, followed by adding 10 g suspended  $\text{Fe}_3\text{O}_4$  nanoparticles into it, after adjusting the pH to 2, a volume of 55 mL formaldehyde was quickly added into the mixture and stirred for 12 h. The obtained urea-formaldehyde (UF) resin coated magnetic composite was washed and dried in vacuum oven. Finally, the UF resin template was burnt out at 280 °C for 2 h to obtain the low cost magnetic porous material.

### 2.2. Grafting of PEI to magnetic porous matrix

Grafting of PEI onto the surface of magnetic porous composite was carried out according to the method described previously with some modifications [20]. Briefly, the magnetic porous composite was firstly activated by 2% methane sulfonic acid to introduce silanol bond, followed by reacting with coupling agent of  $\gamma$ -chloropropyl trimethoxysilane at 80 °C. The treated magnetic porous composite was added into a 10% PEI solution and reacted at 90 °C for 6 h to obtain the expectant adsorbent. The schematic diagram was presented in Fig. 1.

### 2.3. Characterization of adsorbent

The characterization of PEI-grafted magnetic porous adsorbent was conducted by FTIR spectrometer (WQF-410), Field emission SEM (JEOL JSM-6700 F), Zetasizer Nano (ZEN3600, Malvern), Surface Area and Porosity Analyzer (Micromeritics ASAP 2020) and VSM (Nanjing University Instrument Plant).

Adsorbent of 0.01 g was dispersed in 100 mL of 1 mmol/L NaCl solution to sonicate for 15 min. After placing for 24 h, the supernatant was used for zeta potential measurement.

### 2.4. Batch tests

All batch experiments were conducted in duplicates in 100 mL glass conical flask under 150 rpm shaking at room temperature. An amount of 0.05 g adsorbent and 20 mL heavy metal solution was used for every treatment unless otherwise stated. Separation of the

adsorbent was completed in 5 min by applying an external magnetic field. The concentration of heavy metal was determined by atomic absorption spectroscopy (AAS Hitachi Z-8100, Japan) with the mean values reported.

To survey the competitive adsorption among  $\text{Cu}^{2+}$ ,  $\text{Zn}^{2+}$  and  $\text{Cd}^{2+}$ , 0.05 g adsorbent was added into 20 mL multi-metal solution with the initial pH 7. For bi-metal solution, the concentration was 50 mg/L for each and for tri-metal solution, 33.3 mg/L for each metal.

### 2.5. Stability and regeneration of adsorbent

Stability of PEI-grafted magnetic porous adsorbent under acidic and alkaline conditions was evaluated. Briefly, 0.05 g adsorbent was added into 15 mL HCl or NaOH solution with different concentrations, followed by incubating for 6 h, and then they were collected and washed to reach neutral. By determining the magnetic intensity and adsorption ability of the treated adsorbent, stability could be inferred.

To investigate the regeneration, 0.05 g heavy metals loaded adsorbent was treated with 15 mL of 0.02 mol/L EDTA solutions for 15 min. Then the adsorbent was collected and washed for reuse.

## 3. Results and discussion

### 3.1. Preparation and characterization of adsorbent

The magnetic porous powder was consisted of  $\text{SiO}_2$  and  $\text{Fe}_3\text{O}_4$ , in which the main role of  $\text{Fe}_3\text{O}_4$  was to generate magnetism to the powder for separation.  $\text{SiO}_2$  was selected as the matrix to graft PEI due to its good mechanical strength and stability, as well as special surface chemical property for modification [20]. Choosing amorphous porous  $\text{SiO}_2/\text{Fe}_3\text{O}_4$  structure instead of commonly used core shell structure was to get a porous structure with high surface area [11,22]. Therefore, more  $\text{SiO}_2$  was able to contact with PEI for high content graft. The SEM image of magnetic porous composite was displayed in Fig. 2a, with the irregular porous diameter ranging from 500 to 800 nm. However, almost no visible pore was observed after grafting PEI onto the surface (Fig. 2b). This reasonable phenomenon that successful grafting of PEI decreased porous volume was reported by previous researchers [19,23]. Even so, the rough and uneven PEI-grafted magnetic porous composite had a BET surface of 108.5  $\text{m}^2/\text{g}$  and considerably high pore volume of 0.2095  $\text{cm}^3/\text{g}$  (based on Barrett–Joyner–Halenda formula).

### 3.2. FTIR analysis

The infrared spectra related to the adsorbent were shown in Fig. 3. The spectrum of UF resin coated magnetic composite (Fig. 3a) was complex due to various chemical groups in it. The strong peaks at 3354, 1635 and 1252  $\text{cm}^{-1}$  representing N–H stretching vibration, C O (amide I band) stretching vibration and C–N stretching vibration, respectively, might be resulted from the corresponding functional groups presented in the UF resin [15]. After burning out the UF resin, the spectrum for magnetic porous powder was much simple (Fig. 3b). The strong and sharp peak at approximate 1100  $\text{cm}^{-1}$  represents Si–O bond, which also appeared in all other spectra figures. The interrelated peak for Fe–O stretching vibration was appeared at 568  $\text{cm}^{-1}$ , and this characteristic peak took some acceptable changes compared with Fig. 3a. This might be due to the transformation of partial  $\text{Fe}_3\text{O}_4$  to magnetic  $\gamma\text{-Fe}_2\text{O}_3$  [24]. Concomitance with the grafting of PEI onto magnetic porous particles, the spectrum (Fig. 3c) exhibits some changes. The N–H stretching and wagging vibration shifted from 3430 and 800  $\text{cm}^{-1}$  to 3419 and 795  $\text{cm}^{-1}$ , which might be caused by many amine groups in PEI introduced on the surface. The new peaks at 1464 and 1267  $\text{cm}^{-1}$  were attributed to the C–H bending and C–N stretching vibration, respectively, because of the introduction of PEI [23]. It was evident that the FTIR spectra information obtained from Fig. 3a–c accorded with the reaction

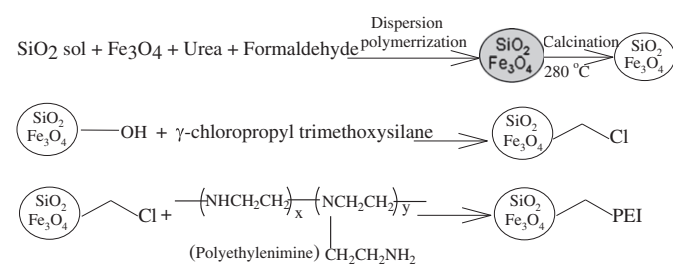


Fig. 1. Schematic depiction of synthesis route for PEI-grafted magnetic porous adsorbent.

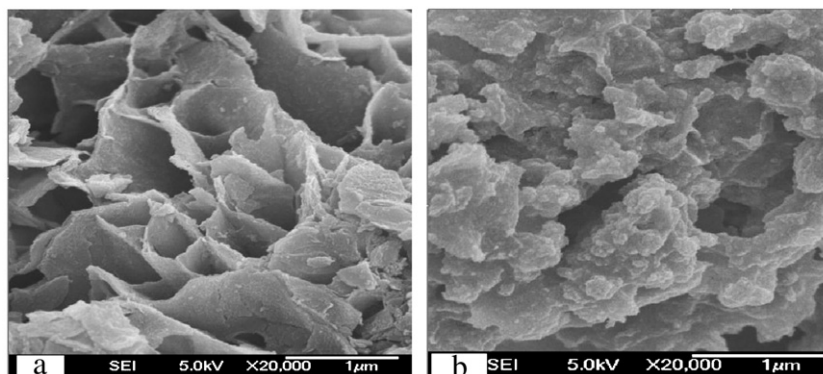


Fig. 2. SEM images of magnetic porous powder (a) and PEI-grafted magnetic adsorbent (b).

process of preparing the PEI-grafted magnetic porous composite, indicating the successful synthesis of adsorbent.

Fig. 3d–f provides the spectra changes of the adsorbent after adsorption of heavy metals. The N–H stretching vibration peak at  $3419\text{ cm}^{-1}$  shifted to  $3421$ ,  $3415$  and  $3427\text{ cm}^{-1}$ , respectively, after  $\text{Cu}^{2+}$ ,  $\text{Zn}^{2+}$  and  $\text{Cd}^{2+}$  uptake. Similarly, the characteristic peak of C–N stretching at  $1267\text{ cm}^{-1}$  and C–H bending at  $1464\text{ cm}^{-1}$  in Fig. 3c varied correspondingly, as shown in Fig. 3d–f. However, two peaks at  $2951$  and  $1631\text{ cm}^{-1}$ , which was attributed to the C–H and C=O (amide I band) stretching vibration presented no change in Fig. 3c–f, suggesting that the adsorption of heavy metals adsorbed on PEI-grafted adsorbent had no direct correlation with the two groups.

### 3.3. Effect of solution pH

The surface charge and the protonation degree of adsorbent were significantly influenced by the pH value, additionally; the speciation of the sorbate was relevant to it [15]. As depicted in Fig. 4a, the removal efficiency increased with the increase of solution pH, with 98%, 80% and 78% efficiency reached for  $\text{Cu}^{2+}$ ,  $\text{Zn}^{2+}$  and  $\text{Cd}^{2+}$  at pH 6.5. Taking into consideration the occurrence of metal hydroxide precipitation under high pH solution, pH at 6 to 7.5 was feasible for effective adsorption of heavy metals in this work.

At low pH value, large amounts of  $\text{H}^+$  might compete with metal ions for the binding site, resulting in the decrease of divalent metal ions binding. Besides, the adsorbent had an isoelectric point at pH 11.8 as detailed in Fig. 4b, which meant the adsorbent surface was positive

charged at  $\text{pH} < 11.8$ . From the electrostatic interaction point of view, the strong electrical repulsion force between adsorbent and metal cations at low pH was able to hinder the metal ions from contacting the PEI-grafted adsorbent surfaces [16,25]. With the increase of solution pH, the electrical repulsion force and competition from  $\text{H}^+$  became weaker, thus the adsorption of metal ions increased. The three trend lines in Fig. 4a presented similar curvature, which suggested that the response sensitivity of heavy metal ions toward the pH change was similar. It was found that at any fixed pH value, the removal efficiency for the three metal ions was  $\text{Cu}^{2+} > \text{Zn}^{2+} \approx \text{Cd}^{2+}$ , implying the stronger affinity of the adsorbent for  $\text{Cu}^{2+}$  than  $\text{Zn}^{2+}$  and  $\text{Cd}^{2+}$ .

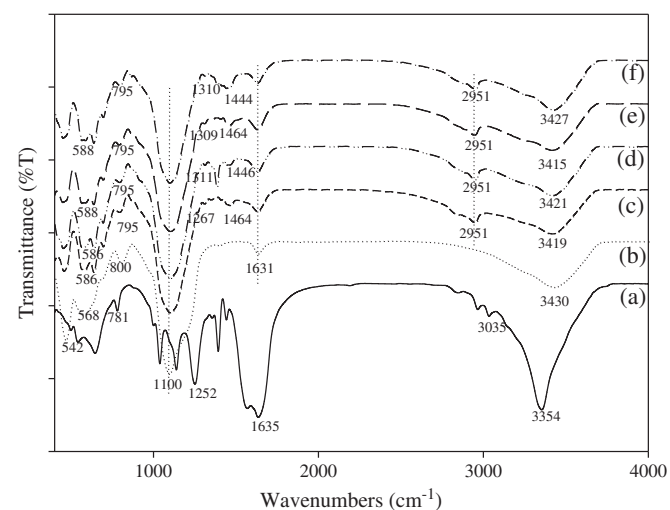


Fig. 3. FTIR spectra: (a) UF resin coated magnetic powder; (b) magnetic porous powder; (c) PEI-grafted magnetic porous adsorbent; (d)  $\text{Cu}^{2+}$  loaded adsorbent; (e)  $\text{Zn}^{2+}$  loaded adsorbent; (f)  $\text{Cd}^{2+}$  loaded adsorbent.

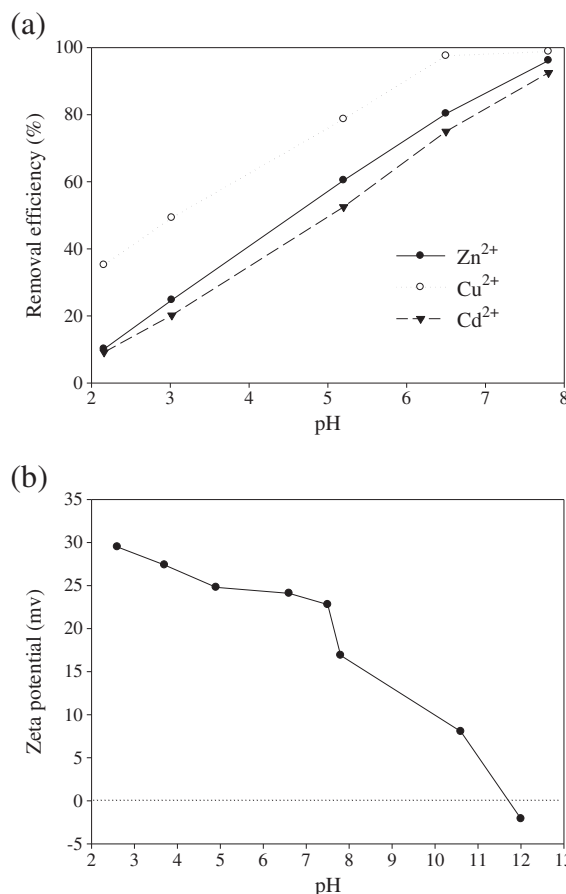


Fig. 4. Effect of pH on adsorption of  $\text{Cu}^{2+}$ ,  $\text{Zn}^{2+}$  and  $\text{Cd}^{2+}$  (initial concentration: 100 mg/L, adsorbent dose: 0.05 g, contact time: 30 min) (a); zeta potential of the adsorbent as a function of solution pH (b).

### 3.4. Effect of contact time

The effect of contact time on adsorption of  $\text{Cu}^{2+}$ ,  $\text{Zn}^{2+}$  and  $\text{Cd}^{2+}$  was studied. Fig. 5 showed that the adsorption rate was very fast and achieved adsorption equilibrium within 10 min. The rapid uptake revealed a high affinity between the heavy metals and adsorbent, which was directly attributed to the characters of PEI-grafted magnetic porous adsorbent. The positive charged adsorbent dispersed in solution evenly after grafting PEI, which was favorable to the rapid contacting between heavy metals and the amino active sites. Furthermore, the adsorbent possessed a high pore volume and BET surface area, which also facilitated the accessibility of amine groups for chelating heavy metals [10]. Although, grafting PEI onto porous carrier decreased the porous volume, had become a limitation in previous reports [19,26]. In this work, the existing huge amounts of porous on matrix successfully overcame the defect and adsorption rate was considerably quick.

Adsorption kinetic model not only allows estimation of adsorption rate but also provides insights into rate expression characteristic of possible reaction mechanisms. It was pointed out that pseudo-second-order adsorption model was based on the assumption that the rate-controlling step of chemisorption involved valence forces through sharing or exchange of electrons between adsorbent and adsorbate, was able to better describe the adsorption kinetic [27,28]. Therefore, the model was applied in this work with its expression as

$$dq_t / dt = k_2(q_e - q_t)^2 \quad (1)$$

where  $q_e$  and  $q_t$  (mg/g) is the amount of adsorbed heavy metal at equilibrium and at time  $t$ , respectively,  $k_2$  (g/mg/min) is the rate constant. Taking into account the initial sorption rate  $v_0$  (mg/g/min)

$$v_0 = k_2 q_e^2 \quad (2)$$

By rearranging the Eq. (1), the following form can be obtained

$$t / q_t = 1 / v_0 + t / q_e \quad (3)$$

As listed in Table 1, the experimental data were in well agreement with the pseudo-second-order model, suggested that the adsorption rate of the heavy metals was controlled by chemical processes. The order of adsorption rates was  $\text{Cu}^{2+} > \text{Zn}^{2+} > \text{Cd}^{2+}$ .

Recently, Chen et al. noted that 120 min was required to reach equilibrium using PEI modified macroporous resin to adsorb 100 mg/L  $\text{Cu}^{2+}$  [23]. Ghoul et al. pointed out that 40 and 120 min were needed, respectively, for 100 mg/L  $\text{Zn}^{2+}$  and  $\text{Cd}^{2+}$  adsorption equilibrium using PEI modified silica gels [19]. Hence, it is remarkable that the PEI modified magnetic porous composite reached equilibrium within

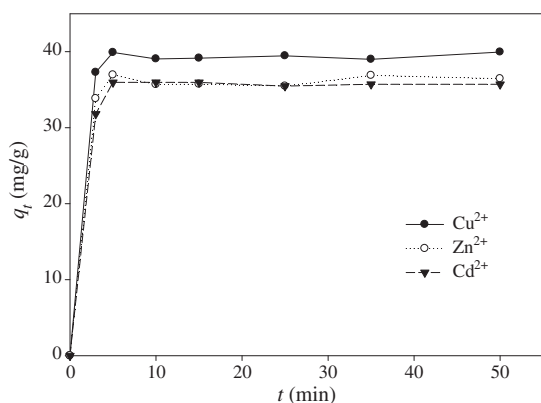


Fig. 5. Effect of contact time on adsorption of  $\text{Cu}^{2+}$ ,  $\text{Zn}^{2+}$  and  $\text{Cd}^{2+}$  (initial concentration: 100 mg/L, adsorbent dose: 0.05 g, pH: 6.5).

Table 1

Adsorption kinetic parameters of  $\text{Cu}^{2+}$ ,  $\text{Zn}^{2+}$  and  $\text{Cd}^{2+}$ , modeled by pseudo-second-order model.

Adsorbate	$v_0$ (mg/g/min)	$k_2$ (g/mg/min)	$q_e$ (mg/g)	$r^2$
$\text{Cu}^{2+}$	192.3	0.121	39.841	0.9997
$\text{Zn}^{2+}$	147.1	0.109	36.634	0.9995
$\text{Cd}^{2+}$	111.1	0.086	35.846	0.9995

10 min compared with other PEI modified adsorbent. It was strongly believed that the magnetic porous matrix was mainly responsible for the rapid adsorption equilibrium. The fast adsorption equilibrium provides an advantage for water treatment system of high effective and roboticized design.

### 3.5. Adsorption isotherms

The adsorption isotherms of  $\text{Cu}^{2+}$ ,  $\text{Zn}^{2+}$  and  $\text{Cd}^{2+}$  with corresponding Langmuir plots were presented in Fig. 6. The Langmuir adsorption model that is based on the assumptions that the adsorption occurs on monolayer and all sites are equal, is often applicable for modeling the adsorption on homogeneous surface sites [28]. Its model is

$$q_e = q_m b C_e / (1 + b C_e) \quad (4)$$

where  $q_e$  (mg/g) is the amount of heavy metals adsorbed at equilibrium,  $C_e$  (mg/L) is the equilibrium solute concentration,  $b$  (L/mg) is the equilibrium constant related to adsorption energy, and  $q_m$  (mg/g) is the maximum adsorption capacity. As listed in Table 2, the maximum adsorption capacity was considerably high, indicating potential application in waste water treatment.

Besides Langmuir model, Freundlich sorption model, which assumes that different sites with several adsorption energies are involved, is widely used for modeling the adsorption occurring on heterogeneous surface sites. It is commonly presented as

$$q_e = K_F C_e^{1/n} \quad (5)$$

where  $K_F$  and  $n$  are the Freundlich constants related to adsorption capacity and adsorption intensity, respectively [32]. The characteristic values for the two models were presented in Table 3.

It could be seen that the Langmuir model was more suitable with the experimental data with the correlation coefficients  $r^2 > 0.98$ , indicated that the adsorbed heavy metal ions formed monolayer coverage on the adsorbent surface. The  $K_F$  and  $n$  ranked in the order of  $\text{Cu}^{2+} > \text{Zn}^{2+} > \text{Cd}^{2+}$ , which was the same with the  $q_m$  order as

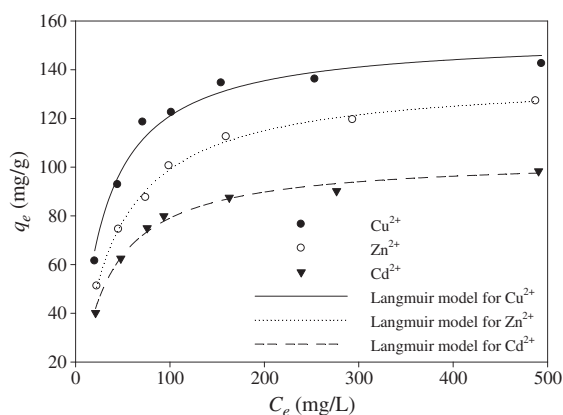


Fig. 6. Experimental metal adsorption isotherms and modeled results using Langmuir equation (initial concentration ranging from 100 to 600 mg/L, adsorbent dose: 0.05 g, pH: 6.5, contact time: 10 min).

**Table 2**  
 $q_m$  values of various adsorbents obtained by Langmuir adsorption model.

Adsorbent	<i>Penicillium simplicissimum</i>	Sugar beet	Amino-Fe <sub>3</sub> O <sub>4</sub> @SiO <sub>2</sub>	Magnetic hydrogels	Acidified clay	Activated carbon	PEI-silica gels	
$q_m$ (mg/g)								
Cu <sup>2+</sup>	61.35	21.3	30.08	117.65	83.3	50.75	–	157.81
Zn <sup>2+</sup>	77.52	17.68	–	–	63.2	56.55	52.08	138.84
Cd <sup>2+</sup>	–	24.39	22.48	140.85	–	48.66	38.46	105.26
Reference	[29]	[28]	[11]	[6]	[30]	[31]	[19]	This work

expected in the kinetic studies. Moreover, this affinity sequence was in agreement with the one deduced from the study of the impact of pH. The accordant conclusions coming from the adsorption kinetic, isotherms and pH study really revealed a differential binding capacity of Cu<sup>2+</sup>>Zn<sup>2+</sup>>Cd<sup>2+</sup>, which would be discussed in Section 3.6.

### 3.6. Competitive adsorption

The competitive adsorption among the studied metal ions was investigated, with the results shown in Fig. 7.

For the tri-metal solution with equal concentration of Cu<sup>2+</sup>, Zn<sup>2+</sup> and Cd<sup>2+</sup>, the corresponding removal efficiency was 96.1%, 36.6% and 33.9%, respectively. For Cu<sup>2+</sup> and Cd<sup>2+</sup> bi-metal solution, the efficiency of Cu<sup>2+</sup> was 63% greater than Cd<sup>2+</sup>. And in Cu<sup>2+</sup> and Zn<sup>2+</sup> mixed solution, the removal of Cu<sup>2+</sup> was double of Zn<sup>2+</sup>. Obviously, in the presence of Cu<sup>2+</sup>, adsorption of Cd<sup>2+</sup> and Zn<sup>2+</sup> was strongly restricted. However, in the bi-metal solution without Cu<sup>2+</sup>, the removal efficiency was relatively high for each (Zn<sup>2+</sup> 60.5%, Cd<sup>2+</sup> 55.7%). These indicated that the PEI-grafted magnetic porous adsorbent had a preferential adsorption of Cu<sup>2+</sup>>Zn<sup>2+</sup>>Cd<sup>2+</sup>. The different adsorption behaviors might be relevant to the nature of metal ionic and the interaction between adsorbent and adsorbate.

It was reported that some linear relationships existed between the rates of complex formation and a variety of properties of the metal ions, such as the atomic radius or the stability constant [28,32]. In this study, the atomic radius (*R<sub>a</sub>*) appeared to reflect the maximum adsorption capacity with the linear relationship shown in Fig. 8a. Furthermore, a linear relationship could be drawn between the initial sorption rate  $v_0$  and the stability constant of amino complex lg  $\beta_3$ , as presented in Fig. 8b. The discoveries indicated that  $q_m$  and  $v_0$  were related with the properties of the heavy metal ions, which might explain the preferential adsorption. And the correlations are able to provide insights into the factors influencing the complex formation, additionally, may allow for prediction of adsorption performance for other metal ions.

### 3.7. Stability and regeneration

The adsorbent was stored in glassware at room temperature when not in use. It was found that the adsorption capacity was almost unchanged under the same operation condition after 127 d storage, which revealed the excellent time stability. As for the degree of acid and alkali resistance, the results were presented in Table 4. It was interesting to observe that the removal efficiency of Zn<sup>2+</sup> decreased after the adsorbent was treated by acid, on the contrary, the removal efficiency increased after alkali treatment.

**Table 3**  
Langmuir and Freundlich parameters for Cu<sup>2+</sup>, Zn<sup>2+</sup> and Cd<sup>2+</sup> adsorption.

	Langmuir model			Freundlich model		
	$q_m$ (mg/g)	$b$ (L/mg)	$r^2$	$K_f$	$n$	$r^2$
Cu <sup>2+</sup>	157.81	0.0318	0.9895	42.561	5.492	0.9248
Zn <sup>2+</sup>	138.84	0.0245	0.9979	33.986	4.405	0.9699
Cd <sup>2+</sup>	105.26	0.0290	0.9956	11.545	2.688	0.8833

It was possible that the PEI-grafted adsorbent was protonated and some H<sup>+</sup> occupied the surface binding sites in the process of acid treatment. Although the treated adsorbent was washed repeatedly to reach neutral for reuse, the influence of acid treatment was irrevocable, resulting in the decrease of removal efficiency. Another possible reason was a few weak grafted PEI released to the solution due to the acid soaking, inducing to the decrease of amino groups [15]. Similarly, after treated by alkali, the surface of the adsorbent was deprotonated, and some functional groups especially hydroxyl might form on the adsorbent surface to chelate metal ions [7], which led to the subsequent increase of removal efficiency.

The magnetization values of all treated adsorbents were strong enough for separation in 5 min, the observation was unexpected. As it was reported that humic acid coated Fe<sub>3</sub>O<sub>4</sub> nanoparticles lost its magnetism completely under 5 mol/L HCl [33], and the dissolution of Fe content on amino-functionalized Fe<sub>3</sub>O<sub>4</sub>@SiO<sub>2</sub> nanomaterial and magnetic zeolites were 100% in 1 mol/L HCl [11,34]. The excellent magnetization stability of this adsorbent could be linked to the nature of magnetic porous matrix and the grafting of PEI. It is believed that the magnetic hybrid matrix possessed certain capability of resisting acid-alkali environment compared with naked Fe<sub>3</sub>O<sub>4</sub> due to the protection of SiO<sub>2</sub> [11]. Besides, in the 280 °C calcination process, some Fe<sub>3</sub>O<sub>4</sub> on the surface converted to  $\gamma$ -Fe<sub>2</sub>O<sub>3</sub> [24], which has similar crystalline structure and similar magnetic properties with Fe<sub>3</sub>O<sub>4</sub>. The formed  $\gamma$ -Fe<sub>2</sub>O<sub>3</sub> on the surface is able to prevent Fe<sub>3</sub>O<sub>4</sub> from further oxidation to maintain stabilities and magnetic properties. Although coating PEI might have decreased the magnetic response, the coated PEI was able to isolate the magnetic material from acid-alkali environment to some extent.

Besides stability, the regeneration of this adsorbent was surveyed by complexing agents of 0.02 mol/L EDTA using Zn ion as the typical heavy metal for study. Fig. 9 shows the removal efficiency of Zn<sup>2+</sup> over four successive adsorption-desorption cycles. It was observed that approximate 95% removal efficiency was reached in the first cycle. Even though the efficiency decreased with the increasing of cycle, over 85% efficiency was obtained in the fourth absorption-

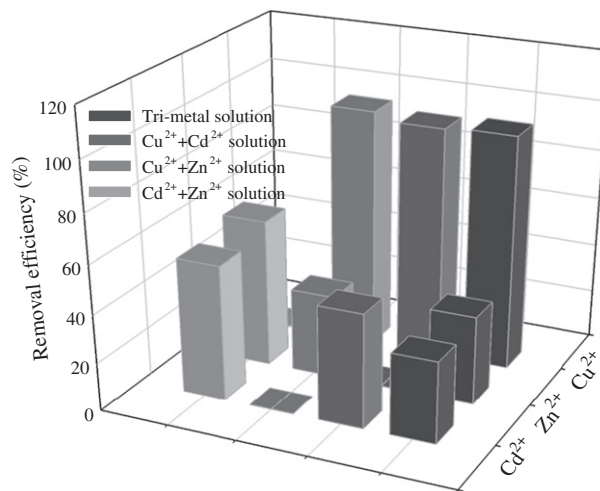


**Fig. 7.** Competitive adsorption of multi-metal solution (adsorbent dose: 0.05 g, pH: 7.0, contact time: 10 min).

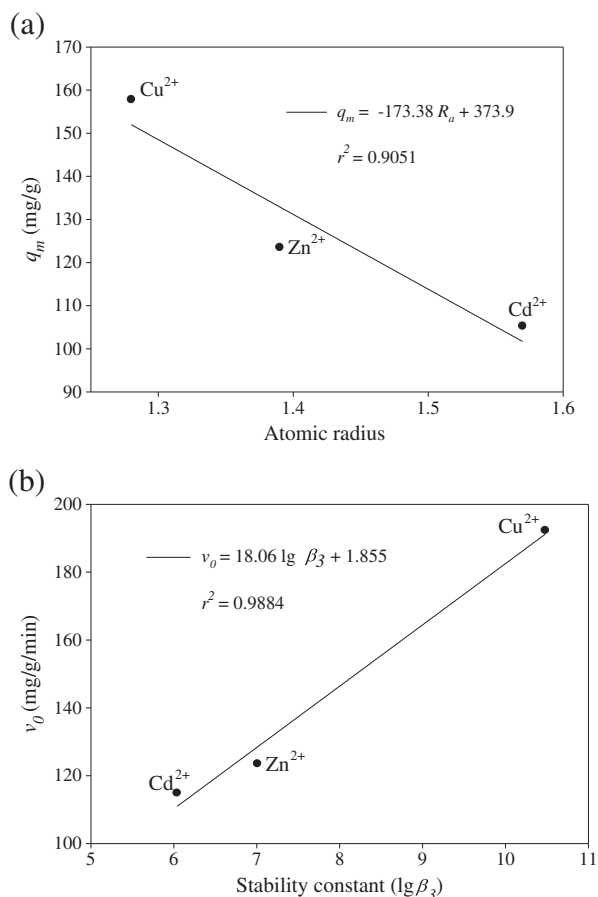


Fig. 8. Relationships between  $q_m$  and atomic radius  $R_a$  (a); between  $v_0$  and stability constant of amino complex  $\lg \beta_3$  (b).

desorption cycle, demonstrating that the prepared adsorbent was cost-effective, and regeneration of it by 0.02 mol/L EDTA solution was quite effective.

#### 4. Conclusions

PEI-grafted magnetic porous adsorbent combining magnetic separation technique and porous properties was developed for removal of heavy metals. The adsorbent possessed excellent magnetization stability in high concentration of acid-alkali environment, as well as fast adsorption equilibrium. These performances were mainly attributed to the properties of magnetic porous powder, indicating the potential of this matrix to combine with other functional materials for developing new adsorbent. The adsorption of  $\text{Cu}^{2+}$ ,  $\text{Zn}^{2+}$  and  $\text{Cd}^{2+}$  was well modeled by pseudo-second-order model and Langmuir sorption isotherm, and the adsorbent presented a preferential binding capacity of  $\text{Cu}^{2+} > \text{Zn}^{2+} > \text{Cd}^{2+}$ . The adsorbent could be used repeatedly by effective regeneration using 0.02 mol/L EDTA solution. Thus it could be concluded that the PEI-grafted magnetic porous adsorbent, with higher uptake capacity and stability, may show great application prospects in heavy metal waste water treatment.

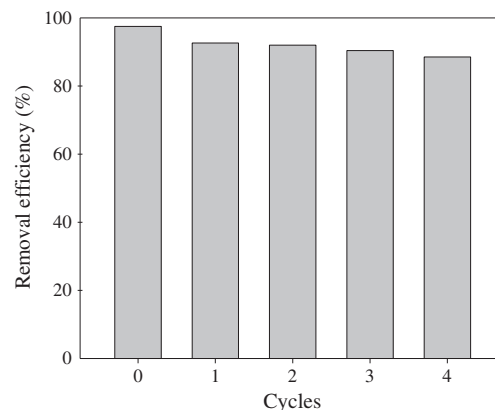


Fig. 9. Four consecutive adsorption-desorption cycles of PEI-grafted adsorbent for  $\text{Zn}^{2+}$  (initial concentration: 100 mg/L, adsorbent dose: 0.05 g, pH 7.5, desorption agent: 15 mL of 0.02 mol/L EDTA).

#### Acknowledgments

This study was financially supported by the Fundamental Research Funds for the Central Universities, Hunan University, the Program for Changjiang Scholars and Innovative Research Team in University (IRT0719), the National Natural Science Foundation of China (50608029, 50978088, 51039001), the Hunan Key Scientific Research Project (2009FJ1010), the Hunan Provincial Natural Science Foundation of China (10JJ7005), the Hunan Provincial Innovation Foundation For Postgraduate (CX2009B080) and the New Century Excellent Talents in University (NCET-08-0181).

#### References

- [1] D.W. O'Connell, C. Birkinshaw, T.F. O'Dwyer, Heavy metal adsorbents prepared from the modification of cellulose: a review, *Bioresour. Technol.* 99 (2008) 6709–6724.
- [2] M.S. Mansour, M.E. Ossman, H.A. Farag, Removal of Cd (II) ion from waste water by adsorption onto polyaniline coated on sawdust, *Desalination* 272 (2011) 301–305.
- [3] L. Tang, G.M. Zeng, G.L. Shen, Y.P. Li, Y. Zhang, D.L. Huang, Rapid detection of picloram in agricultural field samples using a disposable immunomembrane based electrochemical sensor, *Environ. Sci. Technol.* 42 (2008) 1207–1212.
- [4] A.T. Paulino, L.A. Belfiore, L.T. Kubota, E.C. Muniz, V.C. Almeida, E.B. Tambourgi, Effect of magnetite on the adsorption behavior of Pb(II), Cd(II), and Cu(II) in chitosan-based hydrogels, *Desalination* 275 (2011) 187–196.
- [5] K.G. Bhattacharyya, S.S. Gupta, Adsorption of a few heavy metals on natural and modified kaolinite and montmorillonite: a review, *Adv. Colloid Interface Sci.* 140 (2008) 114–131.
- [6] X.J. Ju, S.B. Zhang, M.Y. Zhou, R. Xie, L.H. Yang, L.Y. Chu, Novel heavy metal adsorption material: ion-recognition P(NIPAM-co-BCAm) hydrogels for removal of lead(II) ions, *J. Hazard. Mater.* 167 (2009) 114–118.
- [7] D. Sud, G. Mahajan, M.P. Kaur, Agricultural waste material as potential adsorbent for sequestering heavy metal ions from aqueous solutions: a review, *Bioresour. Technol.* 99 (2008) 6017–6027.
- [8] G.Q. Chen, W.J. Zhang, G.M. Zeng, J.H. Huang, L. Wang, G.L. Shen, Surface-modified *Phanerochaete chrysosporium* as a biosorbent for Cr(VI) contaminated wastewater, *J. Hazard. Mater.* 186 (2011) 2138–2143.
- [9] H.J. Shipley, S. Yean, A.T. Kan, M.B. Tomson, Adsorption of arsenic to magnetite nanoparticles: effect of particle concentration, pH, ionic strength and temperature, *Environ. Toxicol. Chem.* 28 (2009) 509–515.
- [10] Z.L. Wang, X.J. Liu, M.F. Lv, J. Meng, A new kind of mesoporous  $\text{Fe}_7\text{Co}_3$ /carbon nanocomposite and its application as magnetically separable adsorbent, *Mater. Lett.* 64 (2010) 1219–1221.
- [11] J.H. Wang, S.R. Zheng, Y. Shao, J.L. Liu, Z.Y. Xu, D.Q. Zhu, Amino-functionalized  $\text{Fe}_3\text{O}_4@/\text{SiO}_2$  core-shell magnetic nanomaterial as a novel adsorbent for aqueous heavy metals removal, *J. Colloid Interface Sci.* 349 (2010) 293–299.

Table 4  
Effect of different concentration HCl and NaOH treatment on magnetization and removal efficiency.

	HCl					NaOH					Untreated
Concentration (mol/L)	0.1	0.5	1	2	5	0.5	1	2	5		
Magnetization (emu/g)	29	29.4	27.6	22.1	19.4	30.3	29.5	29.6	29.3	30.1	
Removal %	40	36.3	39.7	36.2	38.4	64.1	65.7	65.4	68.1	59.5	

- [12] K.F. Lam, C.M. Fong, K.L. Yeung, G. McKay, Selective adsorption of gold from complex mixtures using mesoporous adsorbents, *Chem. Eng. J.* 145 (2008) 185–195.
- [13] P.E. Duru, S. Bektas, O. Genc, S. Patir, A. Denizli, Adsorption of heavy metal ions on poly(ethyleneimine)-immobilized poly-(methyl methacrylate) microspheres, *J. Appl. Polym. Sci.* 81 (2001) 197–205.
- [14] A. Denizli, S. Senel, G. Alsancak, N. Tuzmen, R. Say, Mercury removal from synthetic solutions using poly(2-hydroxyethyl-methacrylate) gel beads modified with poly(ethyleneimine), *React. Funct. Polym.* 55 (2003) 121–130.
- [15] S.B. Deng, Y.P. Ting, Characterization of PEI-modified biomass and biosorption of Cu(II) Pb(II) and Ni(II), *Water Res.* 39 (2005) 2167–2177.
- [16] S.B. Deng, Y.P. Ting, Polyethylenimine-modified fungal biomass as a high capacity biosorbent for Cr(VI) anions: sorption capacity and uptake mechanisms, *Environ. Sci. Technol.* 39 (2005) 8490–8496.
- [17] R.R. Navarro, K. Tatsumi, K. Sumi, M. Matsumura, Role of anions on heavy metal sorption of a cellulose modified with poly(glycidylmethacrylate) and polyethyleneimine, *Water Res.* 35 (2001) 2724–2730.
- [18] M. Chanda, G.L. Rempel, Polyethyleneimine gel-coat on silica-high uranium capacity and fast kinetics of gel-coated resin, *React. Polym.* 25 (1995) 25–36.
- [19] M. Ghoul, M. Bacquet, M. Morcellet, Uptake of heavy metals from synthetic aqueous solutions using modified PEI-silica gels, *Water Res.* 37 (2003) 729–734.
- [20] F.J. An, B.J. Gao, Chelating adsorption properties of PEI/SiO<sub>2</sub> for plumbum ion, *J. Hazard. Mater.* 145 (2007) 495–500.
- [21] M. Arkas, D. Tsiourvas, Organic/inorganic hybrid nanospheres based on hyperbranched poly(ethyleneimine) encapsulated into silica for the sorption of toxic metal ions and polycyclic aromatic hydrocarbons from water, *J. Hazard. Mater.* 170 (2009) 35–42.
- [22] Y. Zhang, G.M. Zeng, L. Tang, D.L. Huang, X.Y. Jiang, Y.N. Chen, A hydroquinone biosensor using modified core-shell magnetic nanoparticles supported on carbon paste electrode, *Biosens. Bioelectron.* 22 (2007) 2121–2126.
- [23] Y. Chen, B. Pan, H. Li, W. Zhang, L. Lv, J. Wu, Selective removal of Cu(II) ions by using cation-exchange resin-supported polyethyleneimine (PEI) nanoclusters, *Environ. Sci. Technol.* 44 (2010) 3508–3513.
- [24] Q. Gao, F.H. Chen, J.L. Zhang, G.Y. Hong, J.Z. Ni, X. Wei, D.J. Wang, The study of novel Fe<sub>3</sub>O<sub>4</sub>@γ-Fe<sub>2</sub>O<sub>3</sub> core/shell nanomaterials with improved properties, *J. Magn. Magn. Mater.* 321 (2009) 1052–1057.
- [25] X. Han, Y.S. Wong, M.H. Wong, N.F.Y. Tam, Biosorption and bioreduction of Cr(VI) by a microalgal isolate, *Chlorella miniata*, *J. Hazard. Mater.* 146 (2007) 65–72.
- [26] M. Chanda, G.L. Rempel, Chromium(III) removal by epoxy-cross-linked poly(ethyleneimine) used as gel-coat on silica. 1. Sorption characteristics, *Ind. Eng. Chem. Res.* 36 (1997) 2184–2189.
- [27] A. Murugesan, L. Ravikumar, V. SathyaSelvaBala, P. SenthilKumar, T. Vidhyadevi, Removal of Pb(II), Cu(II) and Cd(II) ions from aqueous solution using polyazomethineamides: equilibrium and kinetic approach, *Desalination* 271 (2011) 199–208.
- [28] Z. Reddad, C. Gerente, Y. Andres, P.L. Cloirec, Adsorption of several metal ions onto a low-cost biosorbent: kinetic and equilibrium studies, *Environ. Sci. Technol.* 36 (2002) 2067–2073.
- [29] T. Fan, Y.G. Liu, B.Y. Feng, G.M. Zeng, C.P. Yang, M. Zhou, H.Z. Zhou, Z.F. Tan, X. Wang, Biosorption of cadmium(II), zinc(II) and lead(II) by *Penicillium simplicissimum*: isotherms, kinetics and thermodynamics, *J. Hazard. Mater.* 160 (2008) 655–661.
- [30] T. Vengris, R. Binkiene, A. Sveikauskaite, Nickel copper and zinc removal from waste water by a modified clay sorbent, *Appl. Clay Sci.* 18 (2001) 183–190.
- [31] K. Wilson, H. Yang, C.S. Seo, W.E. Marshall, Select metal adsorption by activated carbon made from peanut shells, *Bioresour. Technol.* 97 (2006) 2266–2270.
- [32] J. Hu, G.H. Chen, M.C.I. Lo, Removal and recovery of Cr(VI) from wastewater by maghemite nanoparticles, *Water Res.* 39 (2005) 4528–4536.
- [33] J.F. Liu, Z.S. Zhao, G.B. Jiang, Coating Fe<sub>3</sub>O<sub>4</sub> magnetic nanoparticles with humic acid for high efficient removal of heavy metals in water, *Environ. Sci. Technol.* 42 (2008) 6949–6954.
- [34] L.C.A. Oliveira, D.I. Petkowicz, A. Smaniotto, S.B.C. Pergher, Magnetic zeolites: a new adsorbent for removal of metallic contaminants from water, *Water Res.* 38 (2004) 3699–3704.